



Correlation between barrier layer T_g and a thin-film composite polyamide membrane's performance: Effect of chlorine treatment[☆]

Sajjad H. Maruf^a, Dae U. Ahn^a, John Pellegrino^a, Jason P. Killgore^b, Alan R. Greenberg^a, Yifu Ding^{a,*}

^a Membrane Science, Engineering and Technology Center, Department of Mechanical Engineering, University of Colorado Boulder, Boulder, CO 80309-0427, USA

^b Materials Reliability Division, National Institute of Standards and Technology, Boulder, CO 80305, USA

ARTICLE INFO

Article history:

Received 2 December 2011

Received in revised form 27 February 2012

Accepted 3 March 2012

Available online 8 March 2012

Keywords:

Chlorine degradation

Glass transition temperature

Polyamide barrier layer

Thin film composite membrane

ABSTRACT

In this study we report changes in the glass transition temperature (T_g) of the polyamide barrier layer (PBL) of a commercial RO membrane as a function of chlorine treatment in which concentration and pH were systematically varied. The results indicate a monotonic decrease of T_g with increasing exposure time at a given chlorine concentration. Further, both the degree and the rate of T_g decrease vary significantly with both the chlorine concentration and pH value of the aqueous chlorine solution. Moreover, the decrease in PBL T_g correlates well with the reduction in the salt rejection of the membrane, but the magnitude of the correlation is specific to chlorine concentration and pH values.

© 2012 Elsevier B.V. All rights reserved.

1. Introduction

Membranes have become a key technology in generation of potable water in response to increasing societal needs. In particular, membrane-based desalination utilizes thin film composite (TFC) reverse osmosis (RO) membranes, due to their relative energy efficiency, small footprint, and low overall cost. The recent geometric growth in RO desalination has also stimulated efforts to improve the performance of these membranes with respect to higher pressure-normalized flux, lower salt passage, and greater tolerance to oxidative damage due to disinfectant exposure, which is used to minimize biological growth/fouling [1].

A TFC RO membrane generally consists of three layers: a crosslinked polyamide barrier layer (PBL) with a thickness of 200 nm or less, a porous support layer (often polysulfone), and a polyester web (Fig. 1). Both the polysulfone and polyester layers provide mechanical support for the PBL, which provides high permeability of water compared to lower salt passage (high rejection) under high pressure. Often, the continuous operation of these membranes is adversely affected by fouling (scaling) and/or formation of a gel layer (biofouling) on the membrane surface, which leads to a significant reduction in the membrane performance. To

restore their original performance, these membranes are treated with oxidative solutions such as chlorine to remove the foulants. Unfortunately, this periodic “cleaning” procedure chemically degrades the PBL, which leads to a permanent reduction in the ability of the TFC-RO membrane to reject salt [2].

The exact physico-chemical mechanism for the observed membrane degradation remains unclear despite decades of research. Spectroscopic techniques such as FTIR (Fourier transform infrared) and XPS (X-ray photoelectron spectroscopy) have often been used to characterize the chemical changes that occur in the PBL [3–7]. Kawaguchi and Tamura suggested that two chemical processes occur upon chlorine exposure, namely, reversible N-chlorination and irreversible aromatic ring chlorination through “Orton ring arrangement” [8]. Avlonitis et al. suggested a two-step chemical reaction: aromatic chlorination followed by chain scission of the amide links [9]. Such chlorination may cause weakening of intermolecular hydrogen bonds and a resulting increase in chain mobility [6,7]. In addition, atomic force microscopy (AFM), electron microscopy, as well as measurements of zeta potential and contact angle have also been utilized to characterize the morphology and surface energy of these membranes upon chlorine exposure [6,10]. Specifically, contact angle and zeta potential are found to decrease upon chlorine exposure [6], although such results may be membrane specific.

However, studies of the physical properties of the PBL of TFC RO membranes are in general scarce compared to those regarding chemical degradation and performance degradation [11,12]. The current lack of knowledge is largely due to the relative absence of methods that can directly characterize these supported, ultrathin,

[☆] Contribution of NIST, an agency of the US government; not subject to copyright.

* Corresponding author at: Department of Mechanical Engineering, 427 UCB, University of Colorado, 1111 Eng. Drive, Boulder, CO 80309-0427, USA.
Tel.: +1 303 492 2036; fax: +1 303 492 3498.

E-mail address: Yifu.Ding@Colorado.Edu (Y. Ding).

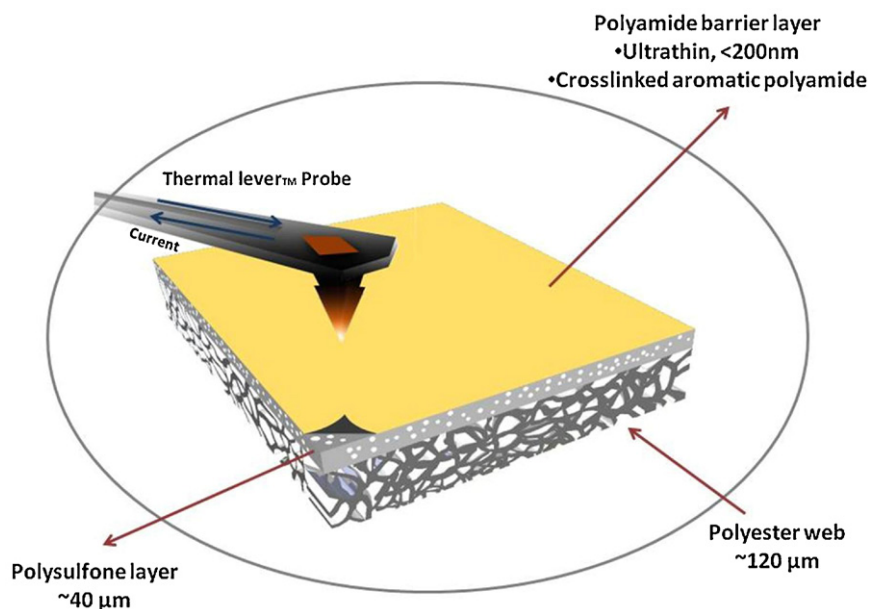


Fig. 1. Schematic illustration of the nano-TA measurement of the polyamide barrier layer atop a TFC RO membrane.

and cross-linked PBLs. Greenberg et al. developed a pendant mechanical analysis (PDMA) technique to characterize the mechanical properties of the interfacially polymerized polyamide layer [13]. However, PDMA cannot be applied to the commercial membranes. It is clear that chlorination and subsequent chemical reactions will inevitably alter the physical properties of the PBL, which in turn will affect salt rejection characteristics [14,15]. Therefore, knowledge of these fundamental PBL physical properties can provide an important link for improved understanding as to how chemical changes in the PBL lead to decreased selectivity of the TFC RO membrane. To address this challenge, we applied a newly developed AFM-based nano-thermal analysis technique (nano-TA) [16], to characterize the evolution of glass transition temperature (T_g) of the PBL for a commercial TFC RO membrane upon controlled chlorine treatments. Further, we evaluated the water and NaCl separation performance for the chlorine-exposed membranes to compare with the T_g measurements. The influences of exposure time, chlorine concentrations, and pH values of the chlorine solutions on the degradation behavior in terms of both barrier layer T_g and the salt rejection of the membrane are reported here.

2. Experimental

2.1. Controlled exposure of TFC RO membranes to chlorine solution

Dow Filmtec XLE-440 membranes,¹ an extra-low-energy, brackish-water TFC RO membrane (Dow Water & Process Solutions) were used in this study [17]. The membrane samples were supplied as rolls of glycerin-dried flat sheets that were stored in a cool and dark environment, as recommended by the manufacturer. The membrane sheets were cut into identical circular pieces (diameter = 4.85 cm) for the filtration experiments, and square pieces (1 cm × 1 cm) for the nano-TA measurements.

¹ Mention of commercial products does not imply recommendation or endorsement by NIST.

The membrane sections were first soaked in 25 vol% aqueous isopropanol (Mallinckrodt, St. Louis, MO) solution for 20 min continuously to remove the glycerin, and then rinsed with running deionized (DI) water for 10 min to remove other impurities [17,18]. These wet membrane sections were immediately immersed in aqueous chlorine solutions, which were then placed in tightly sealed glass vials and protected from light. The chlorine concentrations of the solutions were adjusted by diluting sodium hypochlorite (Scholar Chemistry, used as received) with potassium hydrogen phthalate pH 4 buffer, potassium phosphate monobasic/sodium hydroxide pH 7 buffer and potassium carbonate pH 10 buffer solutions (Fisher Scientific, used as received), and were not monitored throughout the experiments. Specifically, the concentrations of the sodium hypochlorite used in the study ranged from 200 to 20,000 ppm for buffers with pH values of 4, 7 and 10. After soaking in a given chlorine solution for the desired period of time, the membrane sections were removed and then rinsed with DI water for 15 min. The sections were then either immediately used in filtration experiments or completely dried in vacuum oven for the nano-TA experiments.

2.2. Characterization of T_g of the exposed membranes with nano-TA technique

After controlled chlorine exposure and a DI water rinse, sections were dried at 90 °C in a vacuum oven for 12 h to remove absorbed water. These dried sections, along with virgin XLE-440 sections after removing the glycerol and drying as mentioned above, were then characterized by nano-TA, as schematically shown in Fig. 1. Details of nano-TA measurement of supported polymer thin films and TFC RO membranes are described in a recent publication [16]. Briefly, nano-TA is an AFM (Bruker DI3100)-based nanoscale thermal analysis technique (Anasys, Inc.) that utilizes a custom-made thermal lever probe to measure the softening temperature of a material with a spatial resolution of ~100 nm [19,20]. A heating rate of 2 °C/s (120 °C/min) was used for all of the measurements reported in this study. T_g measurements at different locations across the surface of the membranes were carried out for each sample, and the results reported as mean and standard deviation values.

2.3. Filtration experiments on the chlorine-exposed membranes

Filtration experiments with the chlorine-exposed membrane samples were conducted in a Sterlitech HP4750 stirred cell (Sterlitech, WA) with an inner diameter of 3.2 cm and an effective membrane area of 8.48 cm², by use of a constant-pressure, stirred, dead-end (normal flow) filtration configuration. The stirrer power was maintained at a constant value for all measurements. High pressure nitrogen was used to supply the required pressure. All filtration experiments were carried out at room temperature (21 °C). The experimental protocol utilized the following steps. After the controlled chlorine exposure and subsequent DI water rinse, the sample was placed inside the cell, which was then filled with 4000 mL of DI water for the membrane conditioning step recommended by the manufacturer. DI water filtration was carried out at each of three operating pressures, 1.38, 2.07 and 2.76 MPa, for 2 h to ensure complete wetting of the membrane and to leach out/dissolve any remaining preservatives, residual isopropanol, and non-bounded chlorine. The collected permeate was weighed and its conductivity recorded every 10 min throughout the experiment. The conductivity was measured by use of an Ultrameter 6P (Myron L, Carlsbad, CA), and the concentrations were calculated from the conductivity calibration curve prepared for the instrument over an appropriate range of conductivities. After completion of the DI water filtration, the pressure was released, and the DI water feed was replaced with a 2000 mg/L NaCl (Mallinckrodt, St. Louis, MO) solution. Filtration of the salt solution was carried out at an operating pressure of 2.76 MPa, and the collected permeate was weighed every 10 min over a 2 h period. Note that the concentration of the final feed solution after the filtration ranged from 2067 mg/L of the most severely degraded membranes to 2140 mg/L of the least degraded one.

The salt rejection R of the TFC RO membrane samples (as-received or chlorine-treated) was defined as

$$R = \frac{1 - C_p}{C_f}, \quad (1)$$

where C_p and C_f are the salt concentration of the permeate and the feed solutions, respectively. No corrections to the observed rejection, R , were made to account for differences in concentration polarization between membrane samples. Due to the large number of membrane samples and the period required for each filtration experiment, we estimated the uncertainty of the filtration measurements by selecting a single representative membrane sample. Specifically, filtration experiments were repeated three times for those membrane samples exposed to the highest chlorine concentration (20,000 ppm) for the longest duration (2000 min), i.e., having the largest ppmh value (defined later), at each pH solution. As described subsequently, these membrane samples evidenced the largest decrease in performance and T_g , and most likely have the largest uncertainty values because of the severe chlorine exposure.

3. Results and discussion

3.1. T_g Response of the PBL to chlorine exposure

A protocol for PBL T_g measurement by use of nano-TA was established in our previous work [16]. Note that the influence of the polysulfone substrate on the T_g values of the PBL is negligible due to its relatively high T_g and similar thermal conductivity as compared with the PBL [16,21]. As reported, the T_g of the PBL on the virgin (untreated) XLE-440 membrane was determined to be $\sim 172 \pm 4.2$ °C. Fig. 2a shows representative cantilever deflection as a function of temperature from nano-TA measurements of PBL exposed for 2000 min in a 20,000 ppm chlorine solution with a pH value of 7. Each deflection-temperature curve represents a

nano-TA measurement carried out at a randomly selected location on the surface of the PBL. The T_g of the PBL is defined as the temperature at which a significant reduction in deflection occurs (Fig. 2a). As the PBL in contact with the tip is heated to above its T_g , the tip starts to “sink” into the “softened” PBL, causing the change in cantilever deflection reflected in Fig. 2a. For this particular chlorine-treated membrane, the T_g of the PBL was determined to be $\sim 126 \pm 5.6$ °C. Apparently, extended exposure to the chlorine solution significantly reduced the T_g in comparison with that of the virgin membrane ($\sim 172 \pm 4.2$ °C). Note that polysulfone has been reported to be highly resistant to chlorine across a broad pH range [22–25].

Fig. 2b summarizes the T_g of the PBL as a function of chlorine exposure period for five different chlorine concentrations (200, 600, 2000, 6000, and 20,000 ppm) at pH 7 (Fig. 2b). For each chlorine concentration, the T_g of the PBL monotonically decreases with an increase in exposure period, and the magnitude of T_g reduction is greater for higher chlorine concentrations. After long exposure at each concentration, an asymptotic value of T_g is reached with the exceptions of 20,000 ppm and 6000 ppm. Fig. 2c and d shows the changes of T_g after exposure to varying concentrations of chlorine at pH 4 and pH 10, respectively. For chlorine exposure at pH 4, T_g decreases with an increase of chlorine exposure period and concentration. This behavior is similar to that observed at pH 7, but the magnitude of the decrease is lower, particularly at high chlorine concentrations. Specifically, the T_g declined from 172 ± 4.2 °C to 138 ± 4.2 °C after a 4000-min exposure to a 20,000-ppm aqueous chlorine solution. Surprisingly, at pH 10, the degree of T_g reduction appears independent of the chlorine concentration after long exposure, which is quite different from the response observed for pH 7 and pH 4. In addition, the kinetics of the T_g reduction for all chlorine concentrations are noticeably faster at pH 10 than the other pH values.

The Kohlrausch–Williams–Watts equation (KWW), an empirical stretched exponential function, was employed to quantitatively analyze the T_g behavior resulting from chlorine treatment. The KWW equation is given as

$$T_g(t) = T_{g,\alpha} + (T_{g,0} - T_{g,\alpha}) \exp\left(-\left(\frac{t}{\tau_T}\right)^\beta\right), \quad (2)$$

where $T_{g,0}$, $T_{g(t)}$, and $T_{g,\alpha}$ are the measured values of T_g for the virgin PBL, after exposure to a chlorine solution for time t , and the asymptotic value after long exposure, respectively. In addition, τ_T represents the characteristic time scale of the decrease in T_g after chlorine treatment representing how fast it changes with exposure, and β is the so-called stretching parameter, normally ranging from 0 to 1, which characterizes the breadth of the degradation distribution [19,26–28]. Values of KWW parameters were obtained from fitting the experimental data for all of the chlorine exposure results shown in Fig. 2, and these are presented in Table 1. To the best of our knowledge, these are the first reported results for PBL T_g behavior for membranes exposed to chlorine solutions with systematically varying concentration, time and pH. The observed decreases in T_g of the amorphous cross-linked PBL suggest a changes in the structure and physical properties of the polyamide, which would in turn cause a decline in membrane performance.

3.2. Effect of chlorine exposure on membrane permselective behavior

Comprehensive filtration experiments were conducted by use of chlorine-treated XLE-440 membranes in order to examine possible correlation between T_g reduction and separation performance. Chlorine treatment followed the same concentration, pH

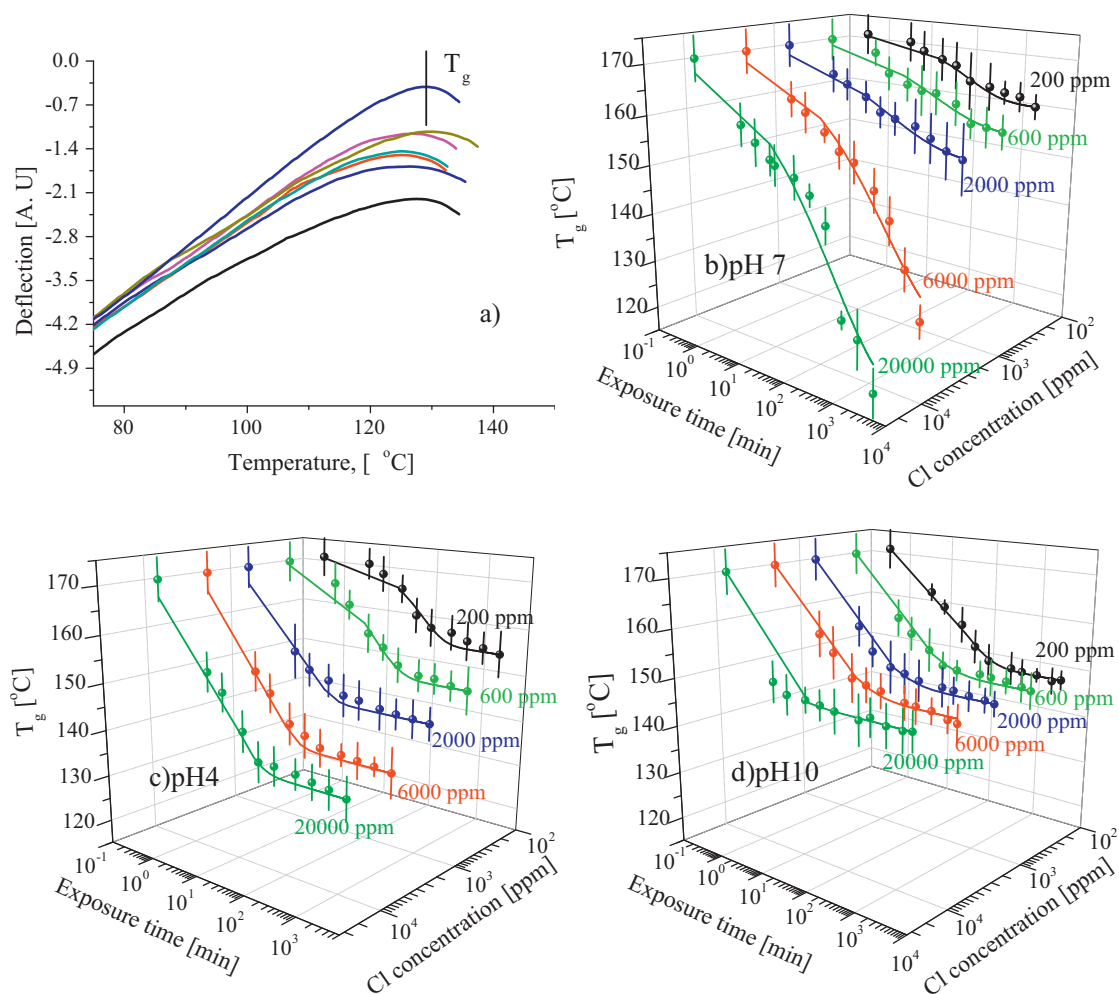


Fig. 2. (a) Deflection of cantilever as a function of temperature from the nano-TA measurements of the PBL after exposure to a chlorine solution (20,000 ppm) for 2000 min with pH 7 buffer. Curves correspond to independent measurements at 7 different locations across the surface of the membrane. T_g of the XLE-440 membrane as a function of exposure period at varying chlorine concentrations at (b) pH 7, (c) pH 4 and (d) pH 10. The data corresponding to different chlorine concentrations were marked on (b)–(d). The curves for each symbol set were fit by use of the Kohlrausch–Williams–Watts (KWW) equation.

and exposure period protocols as employed for the T_g portion of the study. Dead-end flow with a stirred cell was utilized for the study [29]. Permeate flux and salt rejection values of the virgin XLE-440 membrane were measured as 56.52 ± 4.23 L/m²/h and $95.6 \pm 1.2\%$, respectively. The measured permeate flux is within the manufacturer-specified water flux range of 55–81 L/m²/h, while the observed rejection was found to be slightly lower than the manufacturer-specified rejection value of 98.6%. The concentration polarization effect in the dead-end filtration employed is likely greater than would be observed under the cross-flow conditions experienced during operation of a spiral-wound element [30,31]. These differences in flow conditions most likely account for the somewhat lower values of salt rejection. However, this relatively small discrepancy should not have a major effect on the trends

observed with respect to the influence of chlorine exposure on the physical and performance properties.

Fig. 3a shows representative filtration results for a 2000 mg/L NaCl feed solution by use of a XLE-440 membrane sample treated for 50 min in a 200-ppm chlorine solution at a pH 7. The permeate flow rate decreased from ~ 1.21 mL/min to ~ 1.05 mL/min over 2 h. Such reduction in the permeate flow rate can be caused by several factors, including the increase in salinity (osmotic pressure) of the retentate, concentration polarization, and further compaction of the polysulfone support layer after initial DI water filtration [32]. Notably, the observed salt rejection remains rather constant over the 2 h experiments, ranging from $\sim 95.3\%$ to $\sim 94.8\%$ (Fig. 3a). Fig. 3b shows the salt rejection as a function of chlorine exposure period at chlorine concentrations of 200, 2000, and 20,000 ppm, all at a pH

Table 1

KWW parameters of fitted T_g and salt rejection data for chlorine-treated membrane samples as a function of solution concentration and pH values.

Chlorine concentration (ppm)	τ_T (min)			τ_R (min)			$\beta(T_g)$			$\beta(\text{salt rejection})$		
	pH 4	pH 7	pH 10	pH 4	pH 7	pH 10	pH 4	pH 7	pH 10	pH 4	pH 7	pH 10
200	123.7	183.4	40.0	1320.3	1201.3	700.4	0.90	0.64	0.58	0.85	0.78	1
600	62.9	181.0	15.3	–	–	–	0.76	0.45	0.44	–	–	–
2000	13.4	145.7	12.3	317.3	494.9	1224.7	0.75	0.41	0.45	0.45	0.60	1
6000	15.6	834.9	15.5	–	–	–	0.76	0.44	0.46	–	–	–
20,000	22.9	657.0	0.9	199.1	215.5	1325.4	0.71	0.46	0.33	0.39	0.47	1

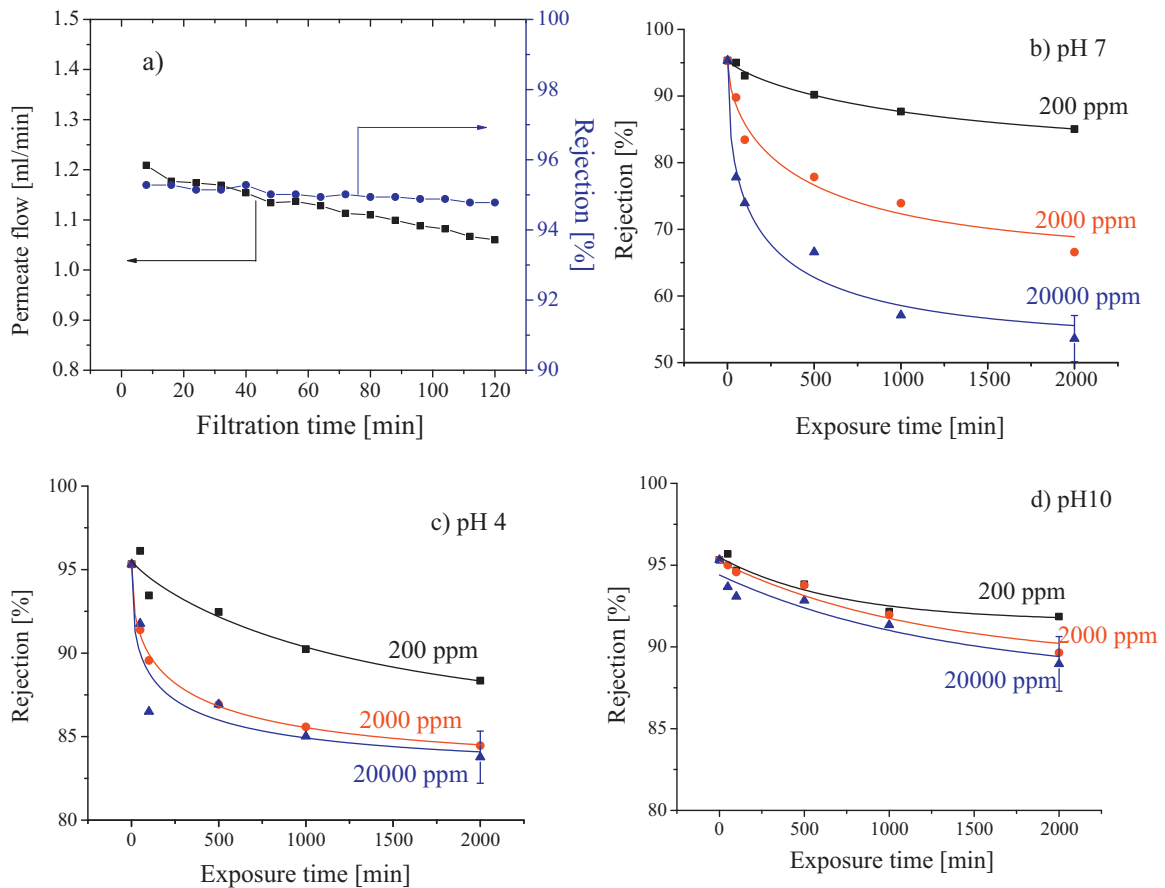


Fig. 3. (a) Permeate (squares) and NaCl rejection (circles) during a 2-h filtration test with a 2000 ppm NaCl feed solution by use of an XLE-440 membrane sample treated in a 200 ppm chlorine solution for 50 min at pH 7. Salt rejection as a function of exposure period at varying chlorine concentrations at (b) pH 7, (c) pH 4 and (d) pH 10. The data corresponding to different chlorine concentrations were marked on (b)–(d). The curves for each symbol set were fit by use of the Kohlrausch–Williams–Watts (KWW) equation.

value of 7. For each chlorine concentration, the salt rejection of the membrane decreases monotonically with an increase in exposure period. For example, the rejection decreases from 95.3% for the virgin membrane to 53.6% after a 2000 min exposure in a 20,000 ppm aqueous chlorine solution. Similarly, Fig. 3c and d shows the salt rejection behavior for membrane samples treated at pH 4 and pH 10. At these pH values, the degree of reduction was less severe for membranes treated for long periods at high concentrations, compared with that at pH 7. In particular, the lowest rejection values observed were 83.8% and 89.0% for samples treated with chlorine solutions at pH 4 and 10, respectively. Aimar et al. showed that degradation in polysulfone and polyvinylpyrrolidone hollow fibers was observed upon oxidative treatment [33,34]. However, these changes showed negligible influence on the filtration characteristics, which reflect the barrier layer properties [35]. Therefore, a substrate effect is unlikely to be a significant factor with respect to the salt rejection characteristics reported in the present work.

Similar to the analysis for T_g , the salt rejection as a function of exposure period was quantitatively described with the KWW equation,

$$R_i(t) = R_\alpha + (R_0 - R_\alpha) \exp\left(-\left(\frac{t}{\tau_R}\right)^\beta\right), \quad (3)$$

where R_0 , $R_i(t)$, and R_α are the rejection values for the virgin membrane, membrane samples treated for time t , and the asymptotic value after long-term exposure, respectively. Here, τ_R represents the characteristic time scale of the performance degradation process. The KWW parameters obtained from fitting the experimental

data are shown in Fig. 3 and presented in Table 1. With an increase in chlorine concentration at pH 4, the overall trend is for a more rapid initial reduction (smaller τ_T and τ_R) in both T_g and salt rejection, although τ_T becomes generally asymptotic for concentrations between 2000 and 20,000 ppm. At pH values of 7 and 10, there were no clear trends in τ_T and τ_R . In contrast, the stretching exponent, β , decreases with the increase of chlorine concentration at for pH 4 and 7 at lower concentrations, and remains around 1 for pH 10. This indicates that the distribution of the chemical/physical processes that lead to the reduction of T_g and membrane salt rejection become increasingly broad with the increase of chlorine concentration, i.e., the complexity of the chemical reactions increases with increasing chlorine concentration.

In the literature, “time–concentration superposition (TCS)” is often applied to collectively describe the effect of exposure period and chlorine concentration [14,30,36]. Fig. 4a presents the measured salt rejection of the XLE-440 membrane as a function of the product of the chlorine concentration and exposure period (in the unit of ppmh). For each pH value, the salt rejection falls reasonably well into a “master curve”, indicating that there may well be some practical advantage in representing degradation phenomena via the TCS approach. Interestingly, there is a clear difference in response among the three values of pH. If salt rejection is taken to represent the degree of membrane degradation, then degradation descends according to pH 7 > pH 4 > pH 10. This trend becomes more evident at higher values of ppmh.

Fig. 4a also includes salt rejection values of chlorine-treated TFC RO membranes reported in literature [3,37,38]. Note that most of

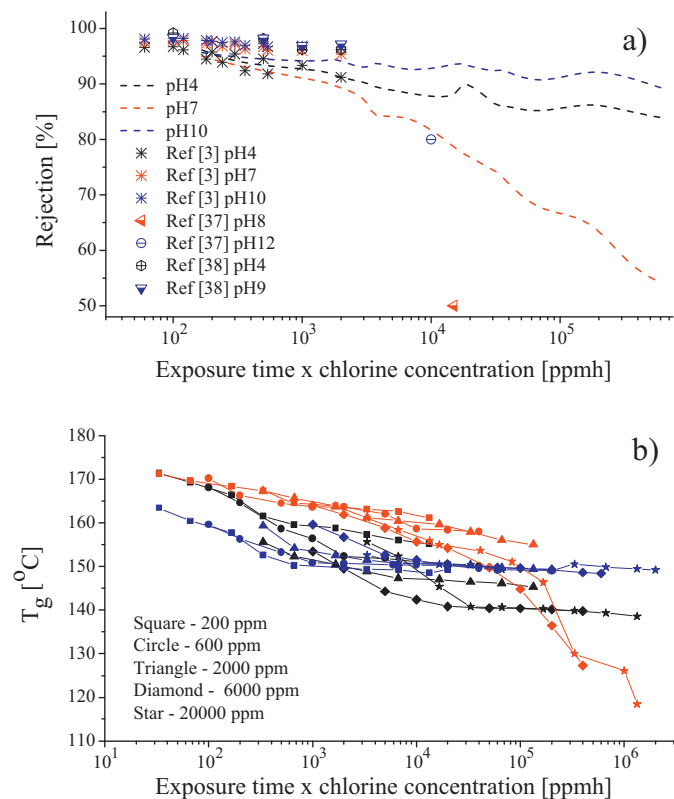


Fig. 4. (a) Salt rejection of the XLE-440 membrane after chlorine exposure as a function of concentration-period (ppmh). Dashed jagged lines represent results from this study, while the other symbols reflect literature data [3,35,36]; symbol colors indicate pH values: black – pH 4, red – pH 7, blue – pH 10; (b) T_g of the PBL of chlorine-treated membranes as a function of concentration-period (ppmh). Different symbols in (b) correspond to membranes treated at different pH values: black – pH 4, red – pH 7, and blue – pH 10. At each pH value, different symbols represent membranes exposed to different chlorine concentrations as listed in (b). (For interpretation of the references to color in this figure legend, the reader is referred to the web version of this article.)

the reported results are from membranes that were treated in a relatively low range of ppmh values. Although from different TFC membranes, these reported salt rejections are generally within the same range as our measurements. However, the pH dependence of the TCS response seems to be membrane-specific. Yuan et al. found that the bdx TFC RO membrane (Hangzhou Beidouxing Membrane Co. Ltd., China.) showed the most severe degradation at pH 4 [3]. In contrast, Raval et al. and Cadotte et al. determined that alkaline conditions cause a greater decrease in rejection than acidic conditions in their experimental TFC RO membranes [37,39]. Kwon et al. observed no noticeable change in salt rejection properties of Filmtec LE membranes upon changing the pH of the chlorine solution treatment [38]. However, more extensive degradation in performance after chlorine treatment at pH 7 as compared to pH 4 and pH 10 conditions with the same FT30-type membrane (similar chemical structure to the XLE-440) has also been reported [40]. It is most likely that the chlorine-induced polyamide degradation/chemical changes depend on the specific chemical composition of the membrane, whereby discrepancies in pH dependence depend upon the specific nature of these changes. Note that the current results (Fig. 4b) encompass a more systematic and broader range of TCS values than those previously reported in the literature.

To better compare the changes in membrane performance represented by the values of salt rejection of the chlorine-treated membranes shown in Fig. 4a with the corresponding changes in the physical properties of the polyamide, PBL values of T_g are presented in Fig. 4b as a function of the product of chlorine concentration

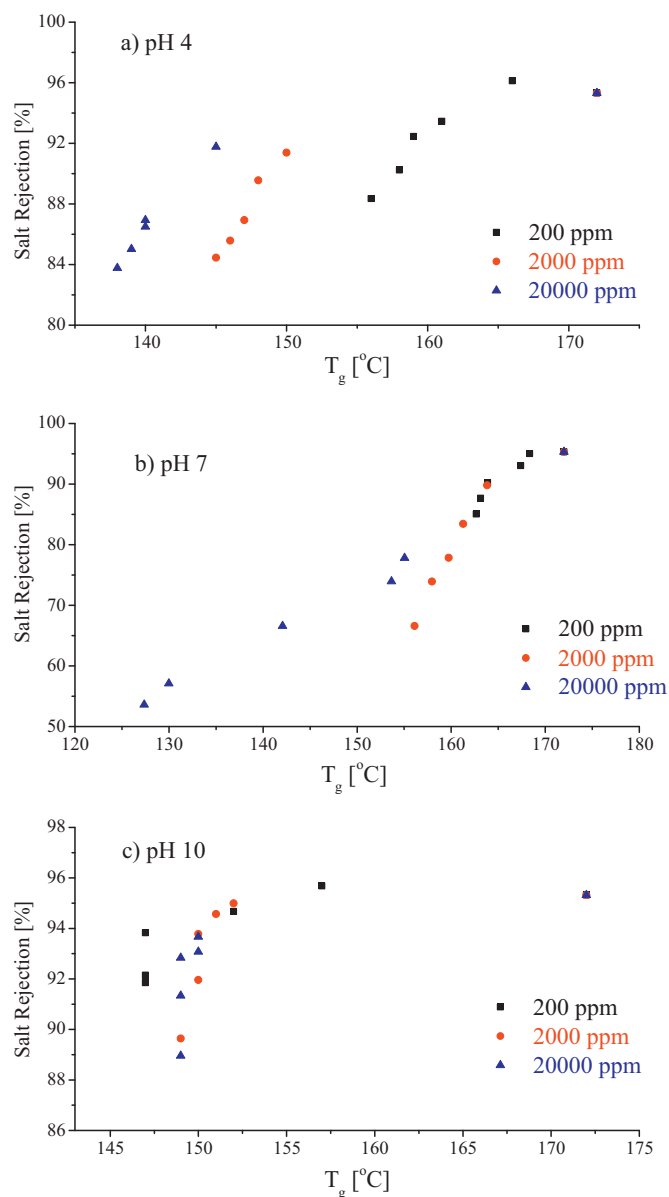


Fig. 5. Relationship between NaCl rejection and PBL T_g for the chlorine-treated XLE-440 membranes as a function of chlorine concentration and pH: (a) pH 4; (b) pH 7, and (c) pH 10. Square, circle, and triangle symbols in (a)–(c) correspond to data from 200, 2000, and 20,000 ppm, respectively.

and exposure time. Overall, the T_g decreases with increasing TCS values in a manner similar to that for the rejection, but the T_g -TCS dependence at pH 4 is somewhat more variable than at pH 7 and pH 10. In addition, a trend towards asymptotic behavior at high TCS values is evident for the pH 4 and pH 10 conditions, whereas T_g values at pH 7 show a more extreme reduction at these high TCS values. This correspondence between the rejection and T_g responses is not surprising, given the underlying chemical changes due to chlorine exposure, even though the T_g was determined for dry PBL while the salt rejection was measured at wet conditions. Evidently, whatever chlorine-induced chemical/structure changes in the membrane should be manifested in both the thermo-mechanical properties (T_g) and transport properties (salt rejection) of the barrier layer.

Correlation between these measures is more directly presented in Fig. 5 in which salt rejection versus T_g is plotted for the chlorine-treated membranes. As expected from the results in Fig. 4, data

in Fig. 5 show that the correlation is positive. In acidic chlorine solutions (pH 4), the curves systematically shift to the left with an increase in chlorine concentration, but the slopes are similar. These characteristics are not maintained for the pH 7 and pH 10 conditions, but concentration sensitivity is clear for the former, yet much less so for the latter.

The ability of the TFC RO membrane to separate the salt and water under pressure is controlled by the difference in the permeability of salt ions and water in the PBL [41–45]. The selectivity of the PBL is often attributed to its “free volume” and/or segmental mobility of the hydrated states [46–49], both of which are directly related to the T_g . Chlorination of polyamide is known to cause a reduction in the strength of the hydrogen bonding [6] and/or hydrolysis of the amide group [50,51]. Such hydrolysis will lead to the reduction of crosslinking density. Each of these factors can lead to a “looser” PBL structure, with a corresponding decrease in T_g and mechanical strength. In particular, such structural changes in the polymer network often lead to the “embrittlement” of the materials, manifested by the reduction in material strength and ductility. Such a trend for chlorine-exposed model polyamides was indeed observed with PDMA measurements [36]. Further, breaking of hydrogen bonding of the polyamide will also lead to the increase of “packing propensity” of the membrane due to the looser structure, as manifested in the pure water filtration experiments [52]. Such “loosened” structures will evidence less selectivity for the water molecules over the salt ions [48].

Several models have been proposed to describe mass transport across the RO membranes [42,53–57], including the widely employed solution-diffusion model [58,59]. By using this model, the permeance of water (represented as A) and salt (B) can be extracted from the filtration experiments to characterize the effect of chlorine treatment on water and salt transport [60,61]. For the analysis,

$$A = \frac{J_w}{(\Delta P - \Delta\pi)} \quad (4)$$

and

$$B = \frac{C_p J_w}{C_m - C_p}, \quad (5)$$

where J_w is the water flux, C_p and C_m are the solute concentration in the permeate and feed side at the membrane surface, respectively, ΔP is the applied filtration pressure, and $\Delta\pi$ is the osmotic pressure across the membrane. The only unknown quantity, C_m , is estimated from

$$C_m = C_b \frac{\exp(J_w/k)}{R_o + (1 - R_o) \exp(J_w/k)}, \quad (6)$$

where C_b is the bulk feed solution concentration, taken as the arithmetic average between the feed and reject compositions, R_o is the membrane intrinsic salt rejection [62], and k is the mass-transfer coefficient obtained from NaCl salt filtration in a similar dead-end filtration configuration [31].

Fig. 6 shows A and B as a function of the product of the chlorine concentration and exposure time (ppmh) for the three pH values employed in this study. At small values of ppmh, A for chlorine-exposed membranes decreases at each of the pH values, compared to that of the virgin membrane (dotted line). As the TCS increases, A increases, but the degree of the increase is pH dependent. In particular, the largest values of A are observed for membranes treated at pH 7. Interestingly, the A values for most of the chlorine-treated membranes are less than that of the virgin value. In contrast, B increases with the increase of TCS at each pH value (Fig. 6b), and the degree of the increase in B is much larger than that of A . However, for lower concentrations at pH 4 B slightly decreases like A at the same pH. Specifically, for the membrane treated at 700,000

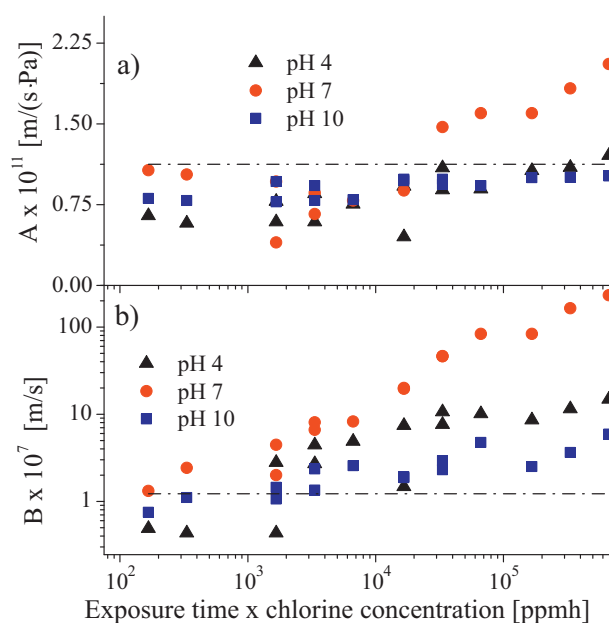


Fig. 6. Transport properties for chlorine-treated XLE-440 membranes during filtration as a function of concentration–time (ppmh) for (a) water permeance A , and (b) salt permeance B . Dash dot lines in (a) and (b) represent the water and salt permeance of a virgin XLE-440 membrane. Triangle, circle and square symbols correspond to membranes treated at pH 4, pH 7 and pH 10, respectively. Chlorine concentrations used were 200, 2000, and 20,000 ppm.

ppmh at pH 7, the A value is about $2\times$ that of the virgin membrane, while B is $250\times$ that of the virgin membrane. As with A , membranes treated at pH 7 show the most dramatic increase in B . The results presented in Fig. 6 indicate that the observed decrease in salt rejection is caused by enhanced salt passage rather than a significant reduction in water permeance.

Water is transported through an RO membrane by a jump diffusion process and so is sensitive to the density of the polymer matrix [42–45,62]. The looser structure due to chemical degradation may reduce the density of the PBL and thus increase the water transport. However, the data in Fig. 6a suggest that any such effect is rather small. In contrast, salt passage is governed by both the steric nature of the free volume and the fixed charge environment in the membrane [46,63,64]. For the case of NaCl, lower mobility of Cl^- relative to Na^+ is the rate-limiting factor for salt permeance [46]. Cl^- diffusion is mostly dominated by the interaction between the anion and carboxylic group ($-\text{COO}-$) in the PBL, and a looser PBL structure will facilitate such interaction, and result in relatively large values for salt diffusion [46]. As pointed out by a reviewer, alternative explanations regarding salt transport have recently been offered [65]. However, even if salt transport occurs via ion pairs [65], a looser PBL structure would still evidence increased mobility (and salt permeance), due to the increase in free volume of the hydrated PBL. The combined effect of these two processes might account for the much higher increase in salt as compared to water transport observed for chlorine-treated membranes. While this study provides new evidence in the form of overall T_g decreases that are compatible with the looser-structure hypothesis, a more extensive study of other PBL compositions is necessary to confirm a general relationship between enhanced salt permeance and T_g reduction.

4. Conclusions

AFM-based nano thermal analysis (nano-TA) was used to measure the T_g of the ultrathin PBL of a commercial TFC-RO membrane and the changes resulting from controlled chlorine exposure.

Results indicate that PBL T_g values decrease with an increase in TCS, i.e., the product of chlorine exposure period and concentration. While the dependence of T_g on TCS varies with the pH value of the chlorine solutions, the reduction in T_g at each pH value appears reasonably correlated with the reduction in salt rejection of the TFC RO membrane. Note that the physico-chemical mechanism underlying the reduction in barrier layer T_g and salt rejection of membranes are currently unclear. Model membrane system, other than commercial membranes, may be more suitable for such mechanistic study. However, these first-ever PBL T_g results not only document the effect of chlorine treatment on commercial membranes, but also provide valuable insights regarding fundamental physical properties of the PBL. Moreover, results of this study suggest that nano-TA might provide an effective addition to standard post-mortem characterization of TFC membranes to quantify the extent of degradation during operation.

Acknowledgement

The authors gratefully acknowledge the National Science Foundation (NSF) Industry/University Cooperative Research Center for Membrane Science, Engineering and Technology (MAST) (formerly Membrane Applied Science and Technology) at the University of Colorado at Boulder (CU-B) for their support of this research via NSF Award IIP 1034720.

References

- [1] A. Antony, R. Fudianto, S. Cox, G. Leslie, Assessing the oxidative degradation of polyamide reverse osmosis membrane—Accelerated ageing with hypochlorite exposure, *J. Membr. Sci.* 347 (2010) 159–164.
- [2] J. Glater, J.W. McCutchan, S.B. McCray, R.M. Zachariah, The effect of halogens on the performance and durability of reverse-osmosis membranes, in: *Synthetic Membranes*, ACS Symposium Series, vol. 153, American Chemical Society, 1981, pp. 171–190.
- [3] G. Kang, C. Gao, W. Chen, X. Jie, Y. Cao, Q. Yuan, Study on hypochlorite degradation of aromatic polyamide reverse osmosis membrane, *J. Membr. Sci.* 300 (2007) 165–171.
- [4] S. Beverly, S. Seal, S. Hong, Identification of surface chemical functional groups correlated to failure of reverse osmosis polymeric membranes, *J. Vac. Sci. Technol.* 18 (2000) 1107–1113.
- [5] C.J. Gabelich, J.C. Frankin, F.W. Gerringer, K.P. Ishida, I.H. Suffet, Enhanced oxidation of polyamide membranes using monochloramine and ferrous iron, *J. Membr. Sci.* 258 (2005) 64–70.
- [6] Y.N. Kwon, J.O. Leckie, Hypochlorite degradation of crosslinked polyamide membranes: I. Changes in chemical/morphological properties, *J. Membr. Sci.* 283 (2006) 21–26.
- [7] Y.N. Kwon, J.O. Leckie, Hypochlorite degradation of crosslinked polyamide membranes: II. Changes in hydrogen bonding behavior and performance, *J. Membr. Sci.* 282 (2006) 456–464.
- [8] T. Kawaguchi, H. Tamura, Chlorine-resistant membrane for reverse osmosis. I. Correlation between chemical structures and chlorine resistance of polyamides, *J. Appl. Polym. Sci.* 29 (1984) 3359–3367.
- [9] S. Avlonitis, W.T. Hanbury, T. Hodgkiess, Chlorine degradation of aromatic polyamides, *Desalination* 85 (1992) 321–334.
- [10] M. Liu, D. Wu, S. Yu, C. Gao, Influence of the polyacyl chloride structure on the reverse osmosis performance, surface properties and chlorine stability of the thin-film composite polyamide membranes, *J. Membr. Sci.* 326 (2009) 205–214.
- [11] N.P. Soice, A.C. Maladono, D.Y. Takigawa, A.D. Norman, W.B. Krantz, A.R. Greenberg, Oxidative degradation of polyamide reverse osmosis membranes: studies of molecular model compounds and selected membranes, *J. Appl. Polym. Sci.* 90 (2003) 1173–1184.
- [12] W. Xie, H. Ju, G.M. Geise, B.D. Freeman, J.I. Mardel, A.J. Hill, J.E. McGrath, Effect of free volume on water and salt transport properties in directly copolymerized disulfonated poly(arylene ether sulfone) random copolymers, *Macromolecules* 44 (2011) 4428–4438.
- [13] V.P. Khare, A.R. Greenberg, W.B. Krantz, Development of pendant drop mechanical analysis as a technique for determining the stress-relaxation and water-permeation properties of interfacially polymerized barrier layers, *J. Appl. Polym. Sci.* 90 (2003) 2618–2628.
- [14] K. Benko, J. Pellegrino, L.W. Mason, K. Price, Measurement of water permeation kinetics across reverse osmosis and nanofiltration membranes: apparatus development, *J. Membr. Sci.* 270 (2006) 187–195.
- [15] I.J. Roh, J.J. Kim, S.Y. Park, Mechanical properties and reverse osmosis performance of interfacially polymerized polyamide thin films, *J. Membr. Sci.* 197 (2002) 199–210.
- [16] S.H. Maruf, D.U. Ahn, A.R. Greenberg, Y. Ding, Glass transition behaviors of interfacially polymerized polyamide barrier layers on thin film composite membranes via nano-thermal analysis, *Polymer* 52 (2011) 2643–2649.
- [17] E.M. Van Wagner, A.C. Sagle, M.M. Sharma, Y.-H. La, B.D. Freeman, Surface modification of commercial polyamide desalination membranes using poly(ethylene glycol) diglycidyl ether to enhance membrane fouling resistance, *J. Membr. Sci.* 367 (2011) 273–287.
- [18] A. Jezowska, T. Schipolowski, G.n. Wozny, Influence of simple pre-treatment methods on properties of membrane material, *Desalination* 189 (2006) 43–52.
- [19] J. Zhou, B. Berry, J.F. Douglas, A. Karim, C.R. Snyder, C. Soles, Nanoscale thermal-mechanical probe determination of 'softening transitions' in thin polymer films, *Nanotechnology* 19 (2008) 495703.
- [20] F. Yang, E. Wornyo, K. Gall, W.P. King, Thermomechanical formation and recovery of nanoindentations in a shape memory polymer studied using a heated tip, *Scanning* 30 (2008) 197–202.
- [21] D. Labahn, R. Mix, A. Schonhals, Dielectric relaxation of ultrathin films of supported polysulfone, *Phys. Rev. E* 79 (2009) 011801.
- [22] A. Freeman, S.C. Mantell, J.H. Davidson, Mechanical performance of polysulfone, polybutylene, and polyamide 6/6 in hot chlorinated water, *Solar Energy* 79 (2005) 624–637.
- [23] G.M. Geise, H.S. Lee, D.J. Miller, B.D. Freeman, J.E. McGrath, D.R. Paul, Water purification by membranes: the role of polymer science, *J. Polym. Sci. B: Polym. Phys.* 48 (2010) 1685–1718.
- [24] H. Park, B. Freeman, Z.B. Zhang, M. Sankir, J. McGrath, Highly chlorine-tolerant polymers for desalination, *Angew. Chem.* 120 (2008) 6108–6113.
- [25] A. Walch, Preparation and structure of synthetic membranes, *Desalination* 46 (1983) 303–312.
- [26] P. Di Martino, G.F. Palmieri, S. Martelli, Molecular mobility of the paracetamol amorphous form, *Chem. Pharm. Bull.* 48 (2000) 1105–1108.
- [27] K. Kawakami, M.J. Pikal, Calorimetric investigation of the structural relaxation of amorphous materials: evaluating validity of the methodologies, *J. Pharm. Sci.* 94 (2005) 948–965.
- [28] S. Yoshioka, Y. Aso, S. Kojima, Usefulness of the Kohlrausch–Williams–Watts stretched exponential function to describe protein aggregation in lyophilized formulations and the temperature dependence near the glass transition temperature, *Pharm. Res.* 18 (2001) 256–260.
- [29] S. Das, P. Saha, G. Pugazhenthii, Modeling and simulation of stirred dead end ultrafiltration process using the Aspen engineering suite, *Ind. Eng. Chem. Res.* 48 (2009) 4428–4439.
- [30] S.T. Mitrouli, A.J. Karabelas, N.P. Isaia, Polyamide active layers of low pressure RO membranes: data on spatial performance non-uniformity and degradation by hypochlorite solutions, *Desalination* 260 (2010) 91–100.
- [31] J. Fernandez-Sempere, F. Ruiz-Bevia, R. Salcedo-Diaz, P. Garcia-Algado, Measurement of concentration profiles by holographic interferometry and modelling in unstirred batch reverse osmosis, *Ind. Eng. Chem. Res.* 45 (2006) 7219–7231.
- [32] R.A. Peterson, A.R. Greenberg, L.J. Bond, W.B. Krantz, Use of ultrasonic TDR for real-time noninvasive measurement of compressive strain during membrane compaction, *Desalination* 116 (1998) 115–122.
- [33] C. Causserand, S. Rouaix, J.P. Lafaille, P. Aimar, Ageing of polysulfone membranes in contact with bleach solution: role of radical oxidation and of some dissolved metal ions, *Chem. Eng. Process.* 47 (2008) 48–56.
- [34] C. Causserand, S. Rouaix, J.P. Lafaille, P. Aimar, Degradation of polysulfone membranes due to contact with bleaching solution, *Desalination* 199 (2006) 70–72.
- [35] S. Rouaix, C. Causserand, P. Aimar, Experimental study of the effects of hypochlorite on polysulfone membrane properties, *J. Membr. Sci.* 277 (2006) 137–147.
- [36] N.P. Soice, A.R. Greenberg, W.B. Krantz, A.D. Norman, Studies of oxidative degradation in polyamide RO membrane barrier layers using pendant drop mechanical analysis, *J. Membr. Sci.* 243 (2004) 345–355.
- [37] J.E. Cadotte, R.J. Petersen, Thin-film composite reverse osmosis membranes: origin, development, and recent new advances, in: *Synthetic Membranes*, ACS Symposium Series, vol. 153, American Chemical Society, 1981, pp. 305–326.
- [38] Y.N. Kwon, C.Y. Tang, J.O. Leckie, Change of membrane performance due to chlorination of crosslinked polyamide membranes, *J. Appl. Polym. Sci.* 102 (2006) 5895–5902.
- [39] H.D. Raval, J.J. Trivedi, S.V. Joshi, C.V. Devmurari, Flux enhancement of thin film composite RO membrane by controlled chlorine treatment, *Desalination* 250 (2010) 945–949.
- [40] S.D. Jons, K.J. Stutts, M.S. Ferritto, W.E. Mickols, Treatment of composite polyamide membranes to improve performance, The Dow Chemical Company (Midland, MI), United States Patent 5,876,602 (1999).
- [41] G. Jonsson, Overview of theories for water and solute transport in 9 UF/RO membranes, *Desalination* 35 (1980) 21–38.
- [42] E.A. Mason, H.K. Lonsdale, Statistical-mechanical theory of membrane transport, *J. Membr. Sci.* 51 (1990) 1–81.
- [43] M. Okazaki, S. Kimura, Selective transport mechanism through the reverse-osmosis membrane, *J. Chem. Eng. Jpn.* 17 (1984) 192–198.
- [44] S. Rosenbaum, W.E. Skien, Concentration and pressure dependence of rate of membrane permeation, *J. Appl. Polym. Sci.* 12 (1968) 2169–2181.
- [45] N.G. Voros, Z.B. Maroulis, D. Marinoskouris, Salt and water permeability in reverse osmosis membranes, *Desalination* 104 (1996) 141–154.
- [46] M.J. Kotlyanskii, N.J. Wagner, M.E. Paulaitis, Atomistic simulation of water and salt transport in the reverse osmosis membrane FT-30, *J. Membr. Sci.* 139 (1998) 1–16.

- [47] H. Eyring, Viscosity, plasticity, and diffusion as examples of absolute reaction rates, *J. Chem. Phys.* 4 (1936) 283–291.
- [48] S.C. George, S. Thomas, Transport phenomena through polymeric systems, *Prog. Polym. Sci.* 26 (2001) 985–1017.
- [49] H. Eyring, T. Ree, Significant liquid structures, VI. the vacancy theory of liquids, in: *Proceedings of the National Academy of Sciences*, vol. 47, 1961, pp. 526–537.
- [50] T. Shintani, H. Matsuyama, N. Kurata, Development of a chlorine-resistant polyamide reverse osmosis membrane, *Desalination* 207 (2007) 340–348.
- [51] R. Singh, Polyamide polymer-solution behavior under chlorination conditions, *J. Membr. Sci.* 88 (1994) 285–287.
- [52] A. Ettori, E. Gaudichet-Maurin, J.C. Schrotter, P. Aymar, C. Causserand, Permeability and chemical analysis of aromatic polyamide based membranes exposed to sodium hypochlorite, *J. Membr. Sci.* 375 (2011) 220–230.
- [53] J.M. Dickson, J. Spencer, M.L. Costa, Dilute single and mixed solute systems in a spiral wound reverse osmosis module Part I: theoretical model development, *Desalination* 89 (1992) 63–88.
- [54] S. Kimura, S. Sourirajan, Analysis of data in reverse osmosis with porous cellulose acetate membranes used, *AIChE J.* 13 (1967) 497–503.
- [55] J. Straatsma, G. Bargeman, H.C. van der Horst, J.A. Wesselingh, Can nanofiltration be fully predicted by a model? *J. Membr. Sci.* 198 (2002) 273–284.
- [56] S. Velikova, A.M. Dave, V. Mavrov, M.H. Mehta, Comparative evaluation of industrial membranes: correlation between transport and operational parameters, *Desalination* 94 (1993) 1–10.
- [57] W. Pusch, Performance of RO membranes in correlation with membrane structure, transport mechanisms of matter and module design (fouling) – state of the art, *Desalination* 77 (1990) 35–54.
- [58] D.R. Paul, Reformulation of the solution-diffusion theory of reverse osmosis, *J. Membr. Sci.* 241 (2004) 371–386.
- [59] G.M. Geise, H.B. Park, A.C. Sagle, B.D. Freeman, J.E. McGrath, Water permeability and water/salt selectivity tradeoff in polymers for desalination, *J. Membr. Sci.* 369 (2011) 130–138.
- [60] H.K. Lonsdale, U. Merten, R.L. Riley, Transport properties of cellulose acetate osmotic membranes, *J. Appl. Polym. Sci.* 9 (1965) 1341–1362.
- [61] Z.V.P. Murthy, S.K. Gupta, Estimation of mass transfer coefficient using a combined nonlinear membrane transport and film theory model, *Desalination* 109 (1997) 39–49.
- [62] J.G. Wijmans, The role of permeant molar volume in the solution-diffusion model transport equations, *J. Membr. Sci.* 237 (2004) 39–50.
- [63] O. Coronell, B.J. Marinas, X. Zhang, D.G. Cahill, Quantification of functional groups and modeling of their ionization behavior in the active layer of FT30 reverse osmosis membrane, *Environ. Sci. Technol.* 42 (2008) 5260–5266.
- [64] E. Peter, Water and salt transport through two types of polyamide composite membranes, *J. Membr. Sci.* 36 (1988) 297–313.
- [65] Jed Pitera, Ting Chen, Young-hye Na, Ratnam Sooriyakumaran, Ankit Vora, Geraud Dubois, Computational modeling of reverse osmosis membrane active layers: structure and transport, in: *North American Membrane Society Annual Meeting*, Las Vegas, NV, June 6, 2011.